

6 Testing lepton universality, the $\pi \rightarrow e\bar{\nu}$ / $\pi \rightarrow \mu\bar{\nu}$ branching ratio

P. Robmann, A. van der Schaaf, U. Straumann, P. Truöl and A. Palladino (guest from PSI/Virginia)

in collaboration with: University of Virginia, Charlottesville, USA; Institute for Nuclear Studies, Swierk, Poland; JINR, Dubna, Russia; Paul Scherrer Institut, Villigen, Switzerland and Rudjer Bošković Institute, Zagreb, Croatia

(PEN Collaboration)

Fundamental fermions (quarks and leptons) are replicated in three families which appear to have a universal coupling strength g to the gauge bosons mediating the electroweak interaction.

Lepton universality is constrained best by the observed value (1) of the branching ratio

$$R_{e/\mu}^{\text{exp}} \equiv \Gamma_{\pi \rightarrow e\bar{\nu}(\gamma)} / \Gamma_{\pi \rightarrow \mu\bar{\nu}(\gamma)} = 1.230(4) \times 10^{-4}. \quad (6.1)$$

The PEN experiment (2) aims at reducing the uncertainty in 6.1 by an order of magnitude which would bring it into the region of the accuracy of the Standard Model prediction. The main component of PEN is a pure-CsI crystal ball shown in Fig. 6.1. Further details on the theoretical motivation and a description of the PEN detection system can be found in the Annual Reports 2006/7.

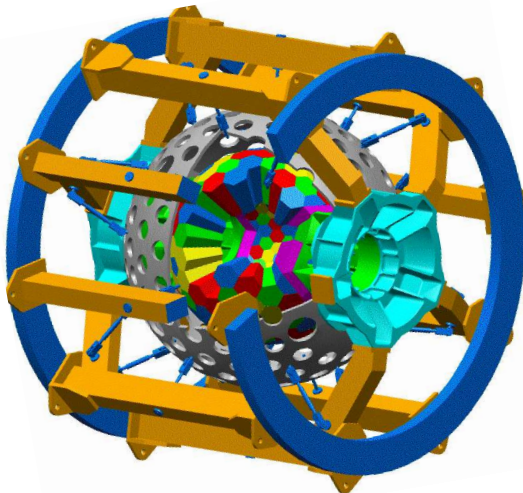


Figure 6.1: The 220 element $\sim 3\pi$ Sr pure CsI spherical electromagnetic calorimeter (see also Fig.6.2).

Whereas $\sim 98\%$ of the $\pi \rightarrow e\bar{\nu}(\gamma)$ decays are unambiguously identified by their positron energy, in the remaining $\sim 2\%$ the observed energy leaks into the region below $m_\mu c^2/2$ dominated by $\pi \rightarrow \mu\bar{\nu}(\gamma)$ followed by $\mu \rightarrow e\nu\bar{\nu}(\gamma)$. For this reason it is crucial to know (measure and/or simulate) the full $\pi \rightarrow e\bar{\nu}(\gamma)$ energy distribution. For this purpose $\pi \rightarrow \mu\bar{\nu}$ events have to be suppressed by many orders of magnitude and the remaining contribution has to be estimated by an analysis of the $\pi \rightarrow e$ time distribution. The suppression is based on the observation of the intermediate 4.1 MeV muon. In order to find the muon for very short pion or muon decay-times and for events in which particles decay before stopping a very precise analysis of the signal waveform from the active pion stopping target has been developed (see last years Annual Report).

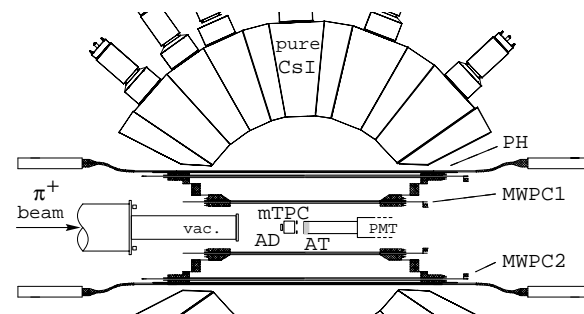


Figure 6.2: PEN setup in the configuration of 2009. CsI: electromagnetic calorimeter (see also Fig. 6.1), PH: plastic scintillator hodoscope, MWPC1/2: cylindrical multi-wire proportional chambers for e^+ tracking, AD: active degrader, mTPC: mini time-projection chamber for π^+ tracking, AT: active target.

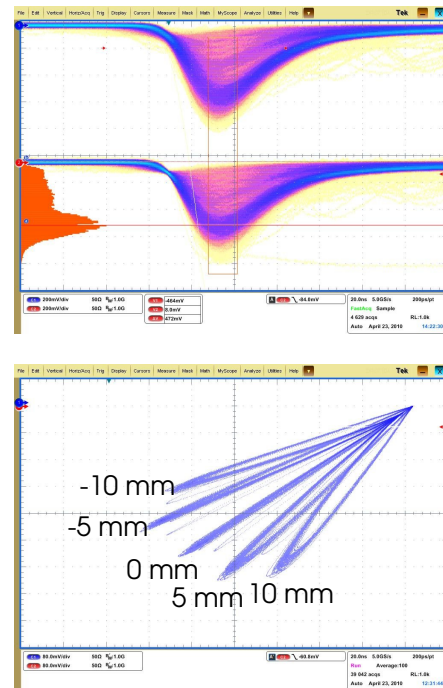
6.1 The new mini-TPC beam tracker

PEN has been taking data during 2008 and 2009 and a final measuring period has been scheduled for the year 2010. During these years, improvements were made, particularly to the beam tracking detector. Figure 6.2 illustrates the setup used in 2009. The signals of all beam detectors are recorded with waveform digitizers. For 2010 the mini-TPC has been replaced by a thin-walled version which will allow us to move the detector closer to the target.

Figure 6.3: Oscilloscope pictures of the signals observed at both ends of a resistive wire of the mini-TPC. The detector was irradiated with a collimated ^{55}Fe source. Both the individual signals (top) and their correlation (bottom) are shown.

In the bottom view the source position along the wire was varied in steps of 5 mm. Signals follow a loop starting and ending at the origin. Central hits result in identical signals which thus populate the diagonal. For off-center hits the relative amplitude deviates most from unity during the rise time. For later times the position dependence fades away so the loops return to the diagonal. For this reason the off-line position algorithm only uses the first ~ 30 ns of the recorded wave forms.

The mini-TPC gives four space points with a resolution of 0.3 mm in vertical (drift) direction and 1 mm in horizontal direction using charge division (see also Fig. 6.3).



6.2 Target waveform analysis

As discussed in great detail in the previous report the target waveform is fit with two different hypotheses. A 2-peak fit assumes a $\pi \rightarrow e\nu$ decay and a 3-peak fit assumes $\pi \rightarrow \mu\nu$ followed by $\mu \rightarrow e\nu\bar{\nu}$. In both fits constraints are

made on the signal amplitudes (deposited energies) which allows a clean separation even when signals appear simultaneous.

Figures 6.4 and 6.5 demonstrate the superb separation obtained with the 2008 data.

Figure 6.4: Distributions of χ^2 values from 2-peak and 3-peak fits to the target waveform for two regions of positron energy. Left: below 60 MeV selects an almost pure sample of $\pi \rightarrow \mu \rightarrow e$ events.

Right: above 60 MeV selects a pure sample of $\pi \rightarrow e\nu$ events.

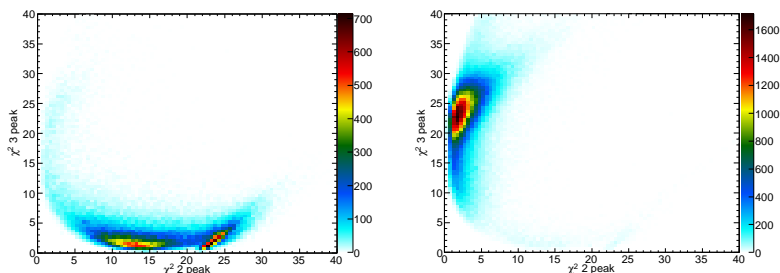


Figure 6.5: The difference in χ^2 of the two fits versus positron energy (left) and decay time (right). The energy region below 50 MeV was pre-scaled by 1:64 in the trigger for data readout.

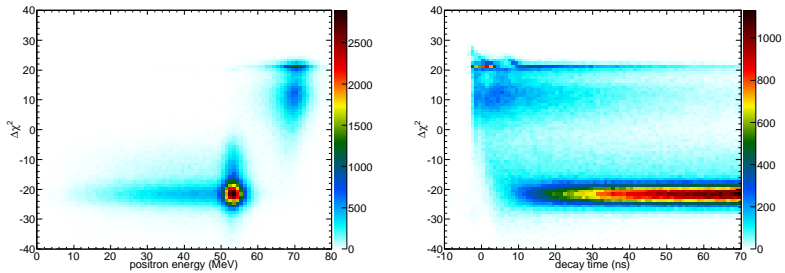
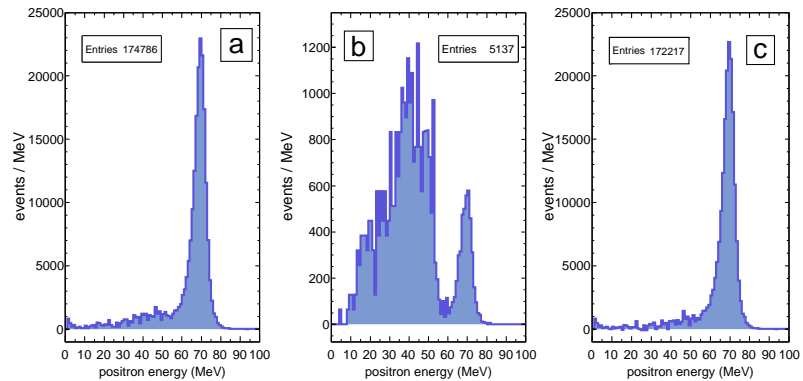


Figure 6.6:

The $\pi \rightarrow e\nu$ positron energy response function from 2008 data. Events are selected with good 2-peak fit. Panel a: events with decay times below 30 ns, panel b: events with decay times 140 - 200 ns, and panel c: the $\pi \rightarrow e\nu$ component in (a) obtained by subtracting muon background extrapolated from (b). A small prompt background remains at very low energy.



6.3 $\pi \rightarrow e\nu$ positron energy response

As mentioned in the introduction, the major source of systematic errors resides in the knowledge of the $\pi \rightarrow e\nu$ energy distribution in the overlap region below 52 MeV. Even when selecting pion decays within 50 ns and even when $\pi \rightarrow \mu\nu$ can be suppressed by four orders of magnitude with the help of the target waveform analysis the overlap region contains similar contributions from the two decay modes and an analysis of the time distribution is required to disentangle them. The analysis is complicated by the contributions from $\pi \rightarrow \mu\nu$ decays just before the pion would have stopped. Figure 6.6 shows the actual state of the art.

6.4 Outlook

Off-line calibration procedures have been finalized and a sophisticated likelihood analysis

based on multi-dimensional probability density functions is being developed. In addition to the two main signal processes, a series of other event types have to be included: radiative decays, in-flight decays, various types of accidental coincidences and pion reactions have been identified so far. It is our aim to determine all probability density functions as much as possible from the measurement but simulations will have to reproduce these results and extrapolate them where necessary.

Whereas data taking will be finished in August 2010 we foresee at least one more year before the result from a blind analysis will become available.

- [1] G. Czapek et al., Phys. Rev. Lett. **70** (1993) 17; D. I. Britton et al., Phys. Rev. Lett. **68** (1992) 3000.
- [2] PEN Collaboration, PSI experiment R-05-01, D. Pocanic and A. van der Schaaf, spokespersons.